ARCHITECTURE CIVIL ENGINEERING ENVIRONMENT
The Silesian University of Technology No. 3/2023

doi: 10.2478/ACEE-2023-0041

THE ANALYSIS OF PILE SKIN AND BASE RESISTANCES INTERACTION BASED ON STATIC PILE LOAD TEST IN EXPERIMENTAL RESEARCH

Krzysztof ŻARKIEWICZ *

*PhD; West Pomeranian University of Technology in Szczecin, Faculty of Civil and Environmental Engineering, al. Piastów 50a, 70-311 Szczecin, Poland
E-mail address: *krzysztof.zarkiewicz@zut.edu.pl*

Received: 23.01.2023; Revised: 07.03.2023; Accepted: 29.03.2023

Abstract
Static pile load tests in laboratory conditions were carried out to study the mechanism of the pile skin and pile base resistance mobilization with settlement and their interactions. The mechanism of the skin resistance at the base is important in the correct interpretation of the pile capacity. Especially in the case of piles shallowly embedded in the bearing layer. In the studies described in this article, high-precision piezoelectric elastic stress maps were used. The tests were carried out on piles with a diameter of 2.5–2.8 cm, and length of 40 cm. Static pile load tests were carried out to measure resistance at the pile base, settlement and change of stress in the soil at the level of the pile base or beneath the pile base were measured. The analysis of stress in soil allowed to investigate the interaction between the resistances of the pile base and skin. The state of stress in the soil close to the pile base, both beneath and above the pile base level was heavily influenced by the simultaneous mobilization of skin and base resistance.

Keywords: **Pile; Pile skin friction; Pile base resistance.**

1. INTRODUCTION

1.1. Piles in engineering practice

Piles transfer the axial loads by skin and base resistance. Pile base resistance is the compression of soil beneath the pile base. Pile skin resistance is completely different from base resistance. Sometimes it is called skin friction, but this friction is observed only at the failure, not in the range of service loads. Before skin friction is achieved the friction is necessary to activate another mechanism of resistance mobilization that comes from the bending of soil space. There are a lot of methods referring to the calculation of pile resistance. Skin friction sometimes refers to the lateral component of the soil stress close to the skin surface. However, in the recent literature one can find another approach based on the bending of soil space close to the pile skin according to Kirchhoff's principles. The intention of this work is not to judge which of the approaches is better, but to present the results of experimental studies that will allow assessing the mechanism of formation of resistance of the skin and pile base.

1.2. Static pile load test and benefits

The most valuable information about pile-soil interaction is the load-settlement relationship. It allows checking the margin of safety and safety factor of pile bearing capacity and the settlement that refers to design loads. This data can be obtained from the static pile load test which is the most reliable test of real pile behaviour under the applied load regardless of layered soil or unknown soil parameters. There are many methods well-known in the literature that allow interpreting pile settlement curves obtained from the static pile load test [1–3]. The mathematical description of the settlement curve with the physical meaning of the parameters described in this function is applied in the Meyer-Kowalow method described widely in [4–7]. A pile load test can be also assimilated with soil investigation allowing to determine soil condition after piling in every place where the pile is installed. This approach allows making deeper investigation of pile load capacity. The settlement curve is the information about the total resistance of the pile including both skin and base resistance together. Separating pile

resistance on skin and base resistance is still a challenge for scientists. This information is crucial because in engineering practice pile load capacity is calculated based on the calculation of skin resistance and base resistance as independent components. There is a question that arise: are the skin friction and base resistance completely independent of each other? This paper aims to consider this phenomenon.

1.3. Model and field test with additional instruments

To obtain information about skin resistance and base resistance pile prepared for the static test should be instrumented in additional sensors. This research is generally based on measurements of strains in pile shafts [8–11]. In these measurements, strain gauges are installed in the core of the pile shaft and provide the data of pile shortening refers to the measured depth which may be then directly used in the calculation of pile axial load changing with depth. In that calculation, the most influential parameter is the elastic modulus of the pile shaft and geometry which is hard to determine especially in piles made in-situ [12, 13]. The last innovation in pile instrumentation apply fibre optic strain gauges allow to determine strains in the pile shaft with good accuracy [12, 14, 15]. Field investigations are valuable because they show real pile-soil interaction. Unfortunately, due to a large number of unknowns and layered soil it is hard to discover all phenomena that occurs during load transferring from the pile to the surrounding soil. Laboratory investigation of static pile load tests, which are presented in [16, 17] cannot be directly compared with natural piles due to small scale but this research can provide a lot of important information about piles behavior.

1.4. Stress in soil and pile technology for the final pile-soil interaction

Besides soil parameters very important in pile-soil interaction are initial stress in soil and stress changes during load increase [18–20]. The previous research [20] pointed out that vertical, horizontal, and shear stress were increasing during the pile load test. Therefore, the geostatic stresses are not relevant to analyze the friction mechanism occurring on the pile's skin. Nevertheless, geostatic stress in the soil is necessary to start the resistance mechanism and friction should be sufficient to mobilize pile skin resistance due to the soil deformation because slipping of soil grains can dramatically decrease or completely stop the skin resistance mobilization. The reason for the different pile load capacities of piles made in different technologies is the influence on the soil state. Some of the technologies especially bored piles may reduce the effective stress in soil and worsen the soil strength, on the other hand displacement piles can improve the soil strength due to the initial radial compression of soil surrounding the pile's shaft. The pile installation effect that was studied in experimental research and numerical approach by [21–23] causes that the soil condition was changed in comparison with previous soil investigations and can rise more difficulties with properly designing of pile load capacity.

1.5. Skin friction and base resistance calculation and interactions

In engineering practice, skin friction and ultimate base resistance are calculated separately using the alfa, beta, lambda method [3] based on soil geotechnical parameters or using CPT soundings which is the direct method that compares CPT cone resistance with pile-soil interaction [24, 25]. The research on pile load capacity carried out in different schemes indicated that base resistance is not the same when friction is not applied in the load transferring and no additional stresses are generated above the level of the pile base [26]. It proves that skin resistance has a positive influence on pile base resistance. On the other hand pile base during static axial pile load test create the zone of stress which surrounds also the pile shaft [27]. The dimensions of that zone and directions of soil movement were presented in [17, 28]. During the pile load test soil is moved also in an upward direction simultaneously affecting the stress above the pile base level as was presented in [29].

2. MATERIALS AND METHODS

2.1. Laboratory stands

The laboratory stand consists of a cylindrical chamber with a diameter of 0.485 m or 0.3 m and a height of 0.6 m, filled up with medium sand. The soil was compacted by tamping in 5 cm thin layers using the same energy of compaction equals 7J. Pile and stress sensors were installed for each test during chamber filling. The chamber with soil, measurement equipment, and the pile was placed in the frame with an installed hydraulic cylinder and independent base for settlement measurements.

The tactile pressure sensor used in the presented experiments consists of two polymeric sheets with pressure-sensitive semiconductive ink printed on each sheet. The active area for measuring was equal to 0.0125 m^2 (dimensions: 111.8 x 111.8 mm) and the

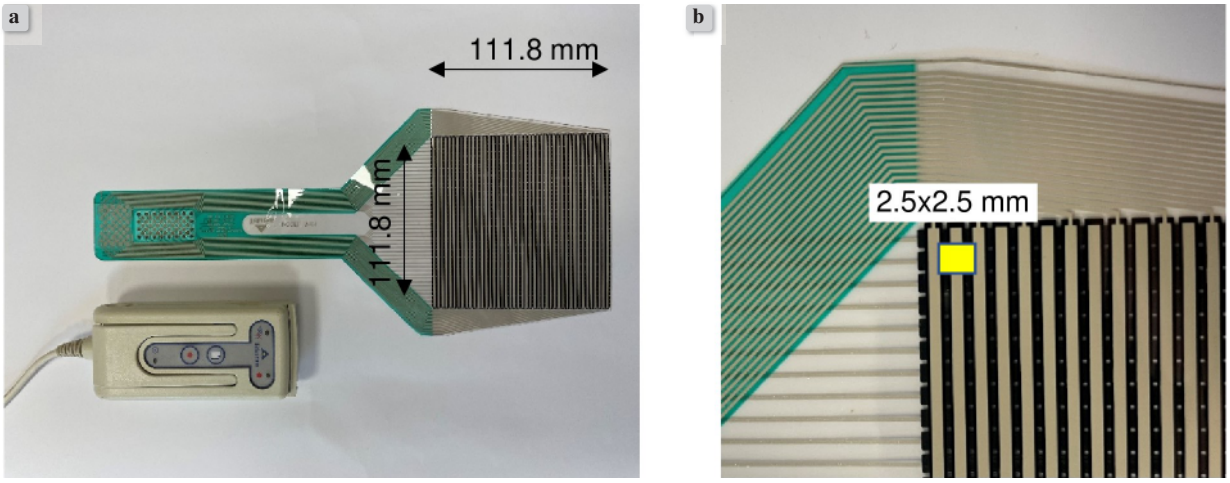


Figure 1.
Pressure mapping system used in measurement stress in soil. a) the sensor with data logger; b) zoom on sensel

thickness was only 0.102 mm. The cross of rows and columns on the sensing area is called sensel, which provides information about the normal force and the localization. The pressure map has 1936 sensels distributed in spacing equal to 2.5 mm. The density of sensels equals 1 per 6.45 mm^2 allows measuring the pressure distribution with high accuracy. The pressure sensor is presented in Fig. 1.

2.2. Soil

The soil used in the laboratory test was classified based on ISO requirements [30] as medium sand MSa. The range of grain size is 0–2 mm with grain uniformity index $C_U = 3.04$ as is presented in Fig. 2. The maximum and minimum porosity index were determined as 0.452 and 0.776, respectively. The water content was in the range 2–5%. The chamber was filled up with soil each time for a new static pile load test. The density was controlled during filing to obtain a homogenous environment, but this information was neglected in the following analysis.

2.3. Piles

In laboratory investigation, two kinds of piles were used: concrete and steel piles. The concrete and steel piles had diameters equal to 0.028 and 0.025 m, respectively and both had lengths equal to 0.4 m, and circular cross-sections. The roughness of used piles was different. Pile 1 had rough skin caused by the pile formed in situ. Pile 2 had smooth skin as it was formed in an elastic PCV tube. Pile 3 and 4 had steel surface which was roughened with a sand-epoxy mixture. Piles were instrumented with compression load cells to measure the force applied at the pile head and resistance at the pile base. The sensor at the pile base had 10.0 mm and 9.6 mm in diameter and height, respectively, and the range of load measurement was 0–10 kN. The laboratory test aimed to carry out research on piles with a ratio of pile length and diameter (14–16) close to the natural piles used in practice, but the presented research does not consider the scale effect more deeply. The pressure maps were placed horizontally in the soil at the level of the

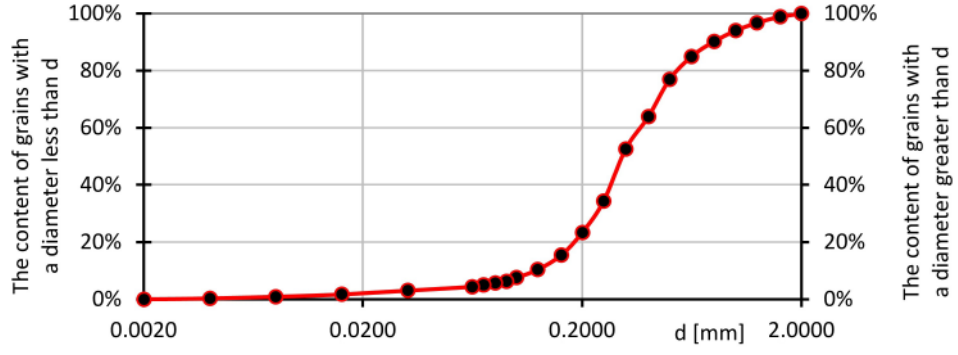


Figure 2.
Grain size distribution of the soil used in the research

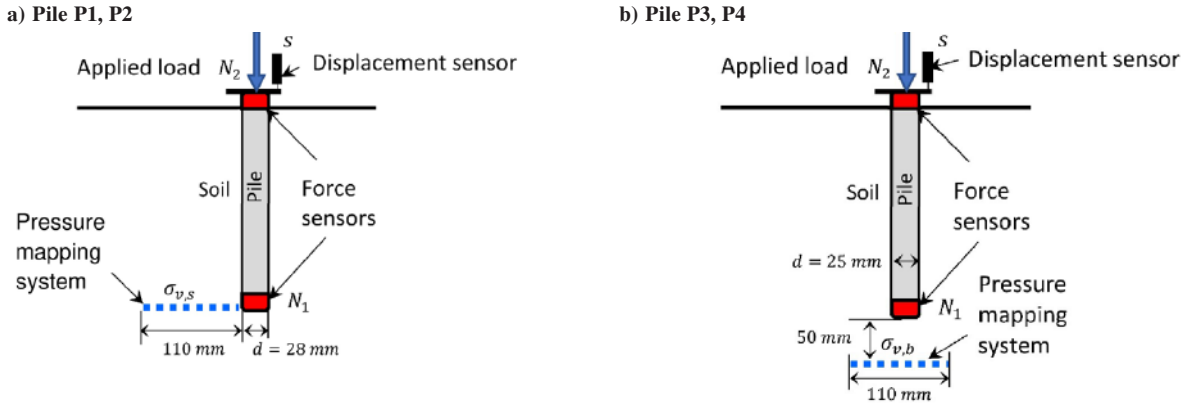


Figure 3.
Schemes of tests with measurement instrumentation

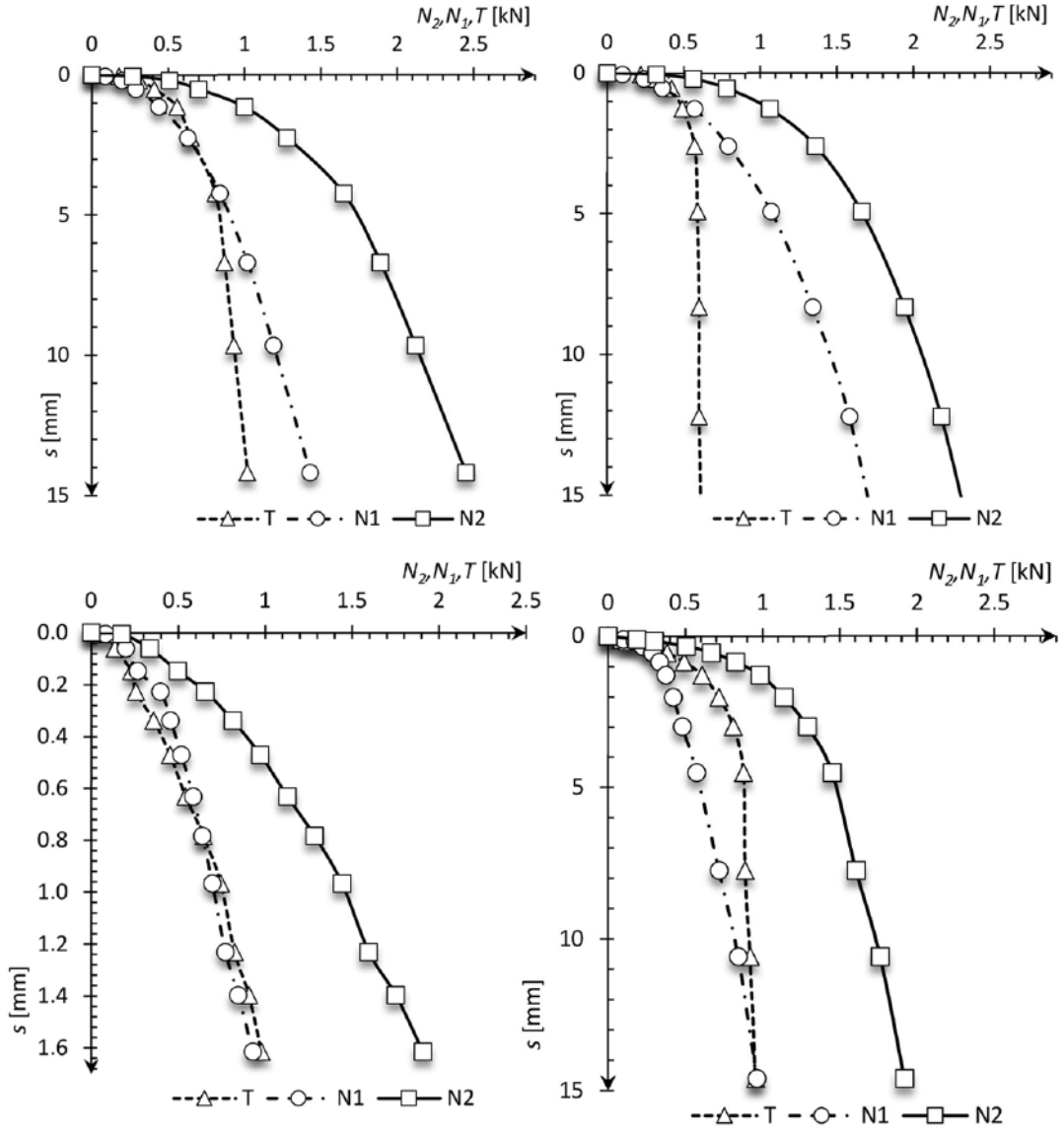


Figure 4.
Outcomes from static pile load test. Where N_2 – axial load applied at pile head, N_1 – pile base resistance, T – pile skin resistance, s – pile head settlement. a) Pile 1, b) Pile 2, c) Pile 3, d) Pile 4

pile base close to the pile skin or 50 mm beneath the pile base refer to piles P1, P2 or P3, P4, respectively as presented in Fig. 3.

3. RESULTS AND ANALYSES

The piles were loaded axially using static load increasing in stages. The time of each stage depended on the stabilization requirements with the assuption that settlement increasing at the same level of applied force should not exceed 0.02 mm per minute. The test was finished when settlement exceeded 30 mm. The following data were measured: applied axial compressive force N_2 [k]; pile head settlement s [mm]; resistance at the pile base N_1 [kN], the vertical component of stress in soil σ_v [kPa]. Outcomes were recorded with a frequency of 1/sec. The results of the static pile load test as the relationship between load in the pile head, base resistance, and skin resistance with the settlement are presented in Fig. 4.

From the laboratory test, four of them were taken for deeper analysis due to the different distribution on pile skin and base resistance. It was observed in Fig.4 that the skin friction of Pile 2 was significantly smaller than other piles. It can result in a smooth pile skin surface in comparison with other piles.

During load tests stress in soil was measured with an interval of 1 second, but only the stress maps referring to the settlement stabilization requirements were taken. The slice of the area with a vertical component of stress in soil, with the scheme of stress measurements as is presented in Fig, 3a, presents Fig. 5a. The stress maps were then presented as the relationship between vertical stress and distance from pile skin as it presented in Fig. 5b. That stresses were approximated with proposed formula (1) which allowed to determine the vertical component of stress in the soil close to the pile skin. The analysis of stress maps allowed to notice that the stresses in the soil in the nearest surroundings at the edge of the pile base were decreasing with the settlement. It could be the pile base resistance that caused greater soil deflection than skin resistance. This phenomenon is very interesting because in some cases pile base may reduce unit skin resistance close to the pile base, but it was not deeply analyzed in this paper. It will be the subject of further research.

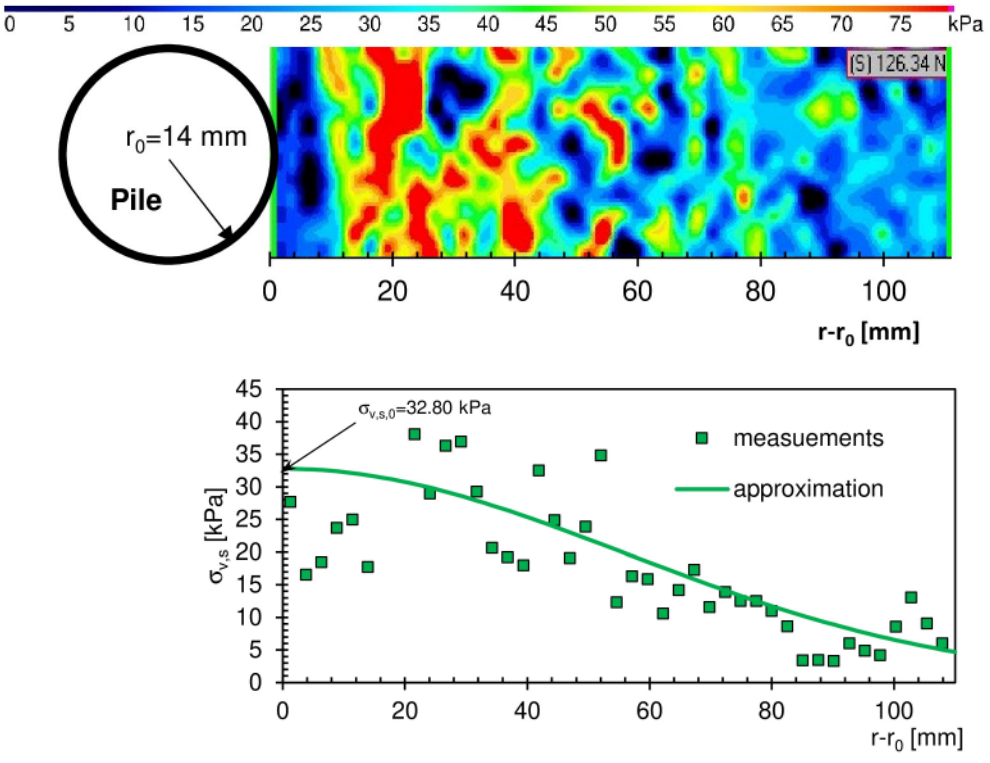


Figure 5.
Example of stress measured by the pressure mapping system of Pile 1 at the load N_2 = 2.18 kN. a) Pressure map from one step of load; b) Outcomes as the average values over a band of vertical component of stress is soil versus distance from pile skin ($r–r_0$) with proposed approximation

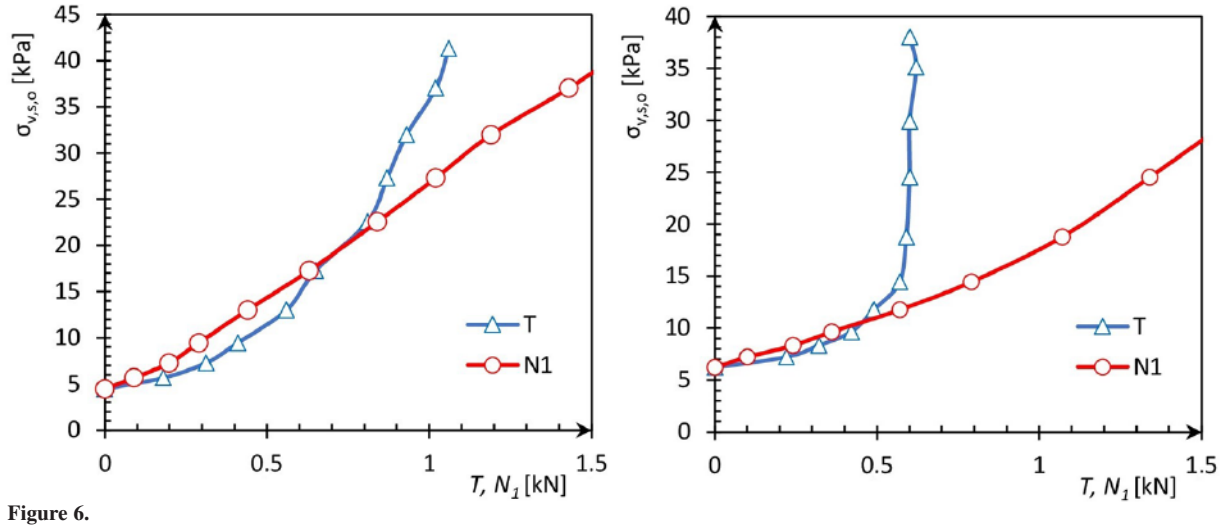


Figure 6.
Stress in soil $\sigma_{v,s,0}$ versus pile skin and base resistance close to the pile skin at the level of pile base where $T=N_2-N_1$. a) Pile 1; b) Pile 2

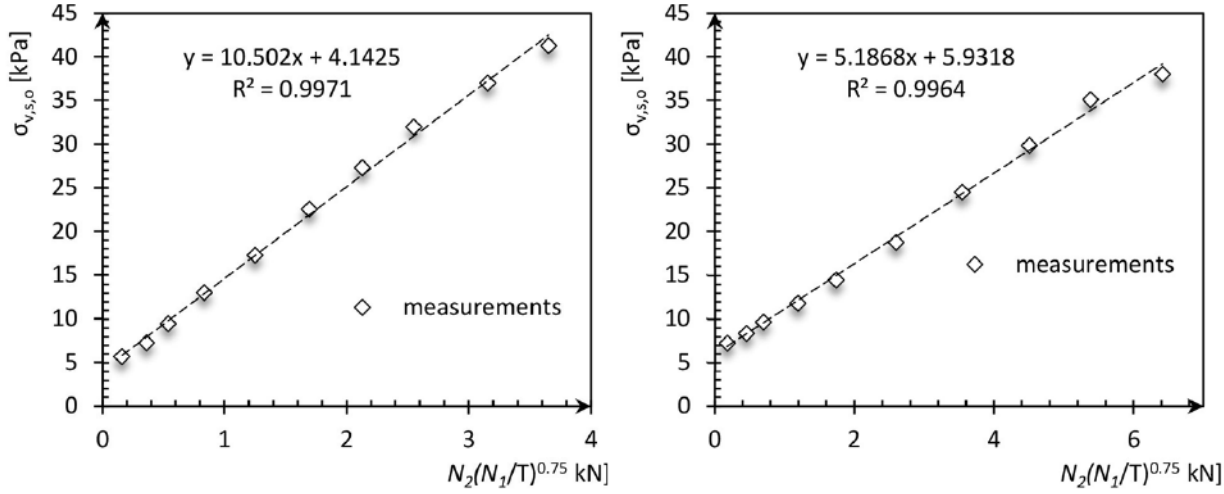


Figure 7.
Calculated stresses v,s,o versus measurements. a) Pile 1; b) Pile 2

Changes in the vertical component of stress in the soil at the level of pile base can be approximated by the suggested Eq. (1)

$$\sigma_{v,s}(r) = \sigma_{v,s,0} exp\left[-C_{s,0}\left(\frac{r-r_0}{r_0}\right)^2\right] \qquad (1)$$

Where:

$\sigma_{v,s,0}$ – vertical component of stress in soil at the skin of pile close to the pile base [kPa];

$C_{s,0}$ – constant [-];

r_0 – pile radius [m];

r – radial distance from pile axis [m].

In every stage of load, the vertical component of stress in soil at the skin of the pile close to the pile base was determined. Results are presented in Fig. 5.

In Fig. 6. stress in soil increased with both base and skin friction resistance mobilization and started from initial geostatic stress. The pile skin resistance of Pile1 with a rough surface was mobilizing with settlement and the relationship was non-linear. Pile 2 with a smooth surface gained ultimate skin resistance which was the result of friction and constant value of friction versus settlement. Although the skin friction was obtained the stresses in the soil surrounding the pile skin were increasing. It was affected by the pile base. Furthermore, the stress in soil versus pile base resistance in the range of skin friction was approximately linear.

The stress in surrounding soil at the level of pile base is influenced by both: skin and base resistance as described by (2).

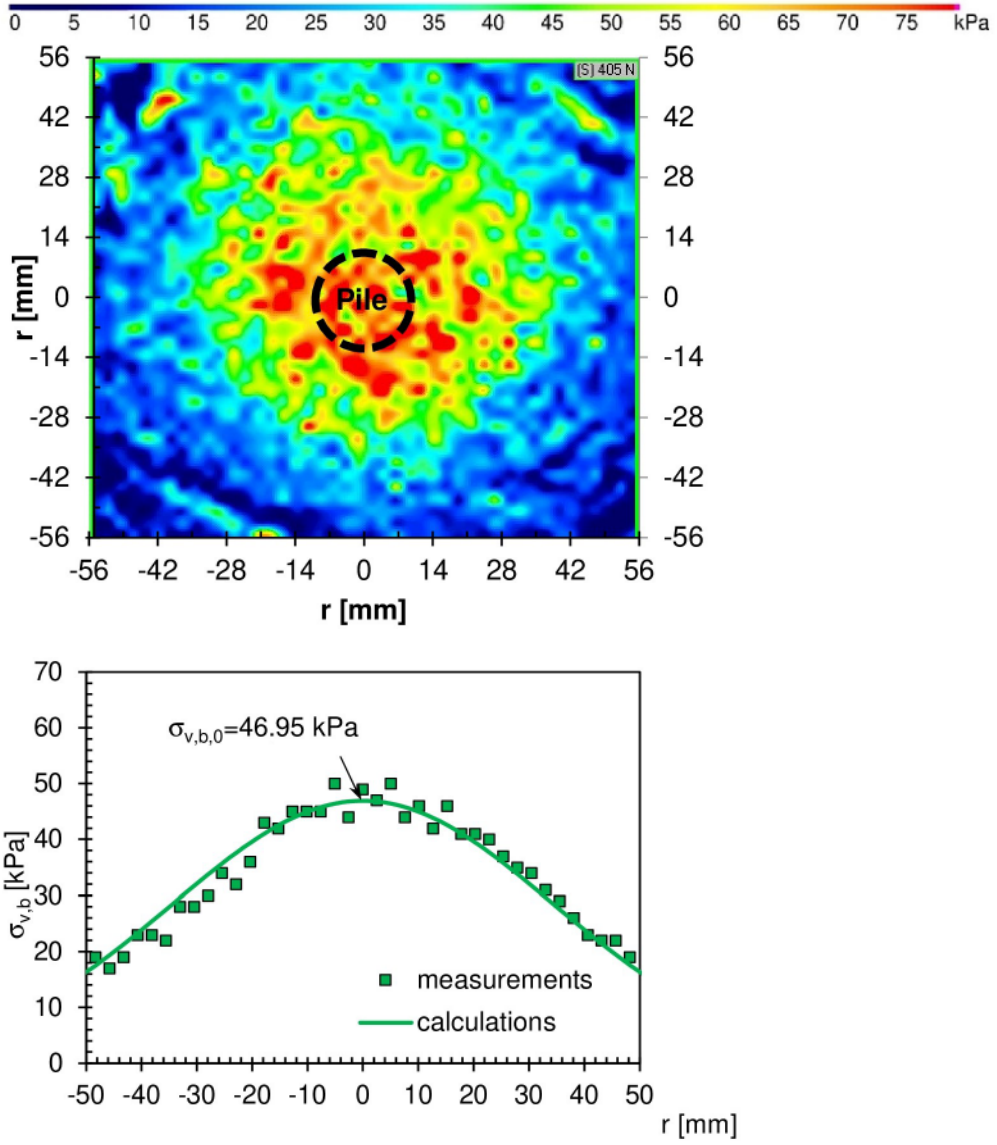


Figure 8.
Example of stress measured by pressure mapping system of Pile 3 as an average over the entire area, at load N_2 =1.91 kN, and settlement s=0.97 mm. a) Pressure map from one step of load; b) Outcomes of the vertical component of stress is soil versus distance from pile axis (r) with proposed approximation

$$\sigma_{v,s,0} = A(N_1 + T)\left(\frac{N_1}{T}\right)^n + \sigma_{v,s,\gamma} \quad (2)$$

Where:

N_1 – pile base resistance [kN];

T – pile skin resistance [kN];

A – parameter obtained from approximation [-];

n – dimensionless statistically determined parameter [-]

Based on the numerical analysis the following equations (3–4) were obtained for Pile 1 and 2:

Pile no 1

$$\sigma_{v,s,0} = 10{,}50(N_1 + T)\left(\frac{N_1}{T}\right)^{0{,}75} + 4{,}14 \quad (3)$$

Pile no 2

$$\sigma_{v,s,0} = 5{,}19(N_1 + T)\left(\frac{N_1}{T}\right)^{0{,}75} + 5{,}93 \quad (4)$$

The fitting of the proposed formula with measurement is presented in Fig. 7.

In tests of Pile3 and Pile4 the stress in soil was measured beneath the pile base. Fig. 8 presents the example of obtained stress maps, and measurement with suggested approximation.

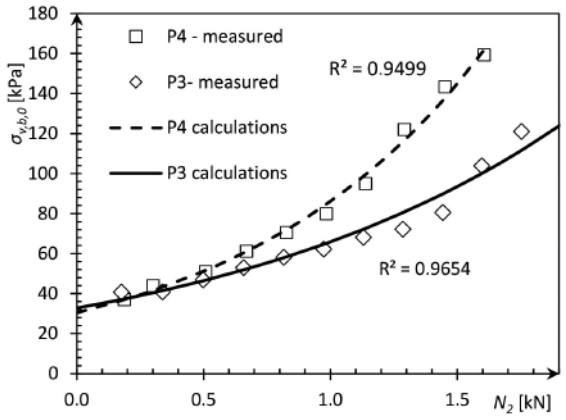


Figure 9.
Stress in soil $\sigma_{v,s,0}$ versus axial force in pile head N_2 50 mm beneath the pile base Pile 3 and Pile 4

Changes in the vertical component of stress in soil beneath pile base can be approximated by Eq. 5

$$\sigma_{v,b}(r) = \sigma_{v,b,0} exp\left[-C_{b,0}\left(\frac{r}{r_0}\right)^2\right] \quad (5)$$

where based on numerical analysis of the proposed curve:

$$C_{b,0} = \frac{3}{2}\left(\frac{r_0}{z_p}\right)^2 \quad (6)$$

where:

r_0 – pile radius [m];

z_p – distance between pile base and installed horizontally pressure maps equal 0.05 m.

Based on Eq. (5-6) the following equation was obtained:

$$\sigma_{v,b}(r) = \sigma_{v,b,0} exp\left[-\frac{3}{2}\left(\frac{r}{z_p}\right)^2\right] \quad (7)$$

For each stage of load, the $\sigma_{v,s,0}$ were determined based on Eq. (7). The stress in surrounding soil at the level of pile base is influenced by both: skin and base resistance. The following relationship was obtained between $\sigma_{v,s,0}$ and N_2 (8).

$$\sigma_{v,b,0} = \sigma_{v,b,\gamma} \exp(BN_2) \quad (8)$$

Where:

B – parameter obtained from approximation [1/kN];

Based on the numerical analysis the following equations (9–10) were obtained for Pile 3 and 4:

Pile no 3:

$$\sigma_{v,b,0} = 32{,}82 \exp(0{,}7N_2) \quad (9)$$

Pile no 4:

$$\sigma_{v,b,0} = 30{,}60 \exp(1{,}0N_2) \quad (10)$$

The measured and calculated stress in soil using Eqs. (9–10) for piles P3, P4 are presented in Fig. 9.

Based on the obtained relationship (3, 4, 9, 10) on stress in the soil the ratio of stresses 50 mm beneath the pile base to the stress at the pile skin at the edge of the pile base was calculated and presented in Fig. 10. The ratio for the analyzed Pile 1 and Pile 2 starts roughly from 25 but instantly falls and stabilize in the range from 5.5 to 11.5.

The analysis indicated that the stress in the soil beneath the pile base is affected by both base and skin friction. Therefore, the following equation (11) was determined.

$$\sigma_{v,b,0} = \sigma_{v,b,0}(N_1) + \sigma_{v,b,0}(T) = \sigma_{v,b,0}(N_1) + \frac{\sigma_{v,b,0}}{\alpha} \quad (11)$$

Where:

α – the parameter of skin resistance influence on stress in the soil beneath the pile base [-]

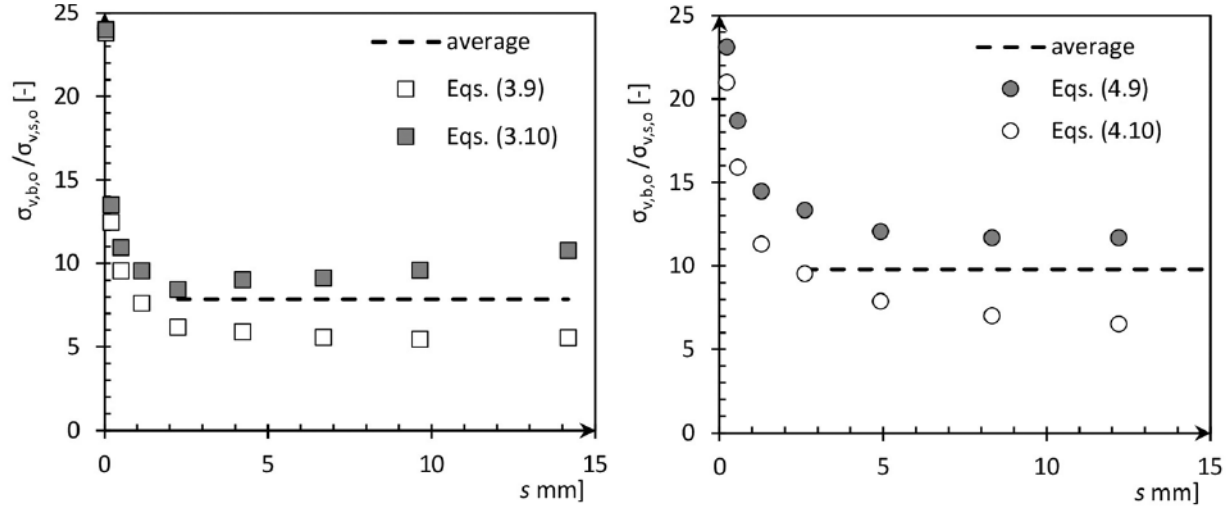


Figure 10.
Calculated ratio of stresses $\sigma_{v,b,0}$ / $\sigma_{v,s,0}$ versus settlement. a) Pile 1; b) Pile 2

$\sigma_{v,s,0}$ (T)=0.04 $\sigma_{v,s,0}$ – at small settlement < 2 mm;

$\sigma_{v,s,0}$(T)=(0.09÷0,18) $\sigma_{v,b,0}$ – at large settlements ≥ 2 mm.

Skin resistance of analyzed piles generated additional resistance beneath the pile base in the range from 4% to 18% of total stress in soil. Ultimate pile base capacity depends on the state of stress therefore skin resistance can improve the pile base capacity. This phenomenon was also observed in previous investigations [26]. On the other hand, pile base resistance has a significant influence on stress in the soil above the pile base level, which was proved in this research. This phenomenon which is also described in the literature [31] may improve the friction mechanism on the pile skin.

4. CONCLUSIONS

The main aim of the research presented in this paper was to analyze the interaction between pile base resistance and skin resistance by the analysis of stresses in soil. Stress in the soil was measured using pressure mapping systems which were previously calibrated to investigate stress in soil. The results of the vertical component of stress in the soil in a test of stress measurements surrounding the pile shaft had a greater variety of stresses beneath the pile base which was caused by the formation of increased stress zones around the pile shaft.

The state of stress in the soil close to the pile base, both beneath and above the pile base level was heavily influenced by the simultaneous mobilization of skin and base resistance.

Skin resistance can improve the pile base capacity due to the stress increasing close to the pile base. Base resistance can increase the stress in the soil above the level of the pile base. Due to the greater stress in soil skin friction can be also improved.

Conclusions were drawn only for the investigations presented in the paper and they are not generalizations for other piles.

REFERENCES

[1] Lastiasih, Y.; Sidi, I.D. (2014). Reliability of Estimation Pile Load Capacity Methods. *J. Eng. Technol. Sci*., 46, 1–16, doi:10.5614/j.eng.technol.sci.2014.46.1.1.

[2] Hasnat, A. (2015). Prithul Saha Ultimate load capacity of axially loaded vertical piles from full scale load test results interpretations applied to 20 case histories., doi:10.13140/2.1.3755.2960.

[3] Wrana, B. (2015). Pile Load Capacity – Calculation Methods. *Stud. Geotech. Mech*., 37, doi:10.1515/sgem-2015-0048.

[4] Meyer, Z. (2017). Wykorzystanie testu statycznego do prognozy osiadania, mobilizacji podstawy i pobocznicy. In Proceedings of the Naprawy i wzmocnienia konstrukcji budowlanych; Wisła, 303–318.

[5] Meyer, Z.; Żarkiewicz, K. (2015). Analiza współpracy pala z gruntem w dużym zakresie osiadania. In Awarie Budowlane; Szczecin-Międzyzdroje, 405–412.

[6] Meyer, Z.; Żarkiewicz, K. (2018). Skin and Toe Resistance Mobilisation of Pile During Laboratory Static Load Test. *Stud. Geotech. Mech*, 40, 1–5.

[7] Siemaszko, P.; Meyer, (2019). Z. Static load test curve analysis based on soil field investigations. *Bull. Polish Acad. Sci. Tech. Sci*., 67, 329–337. doi:10.24425/bpas.2019.128607.

[8] Fioravante, V. (2002). On the shaft friction modeling of non-displacment piles in sand. *Japanese Geotech. Soc*., 42, 23–33, doi:10.1248/cpb.37.3229.

[9] Guo, Z.; Deng, L. (2018). Field behaviour of screw micropiles subjected to axial loading in cohesive soils. *Can. Geotech. J*., 55, 34–44, doi:10.1139/cgj-2017-0109.

[10] Gupta, R.C. (2013). Load-Settlement Behavior of Drilled Shafts in Multilayered Deposits of Soils and Intermediate Geomaterials. *Geotech. Test. J*., 36, 20130016, doi:10.1520/GTJ20130016.

[11] Kim, D.; Jeong, S.; Park, J. (2020). Analysis on shaft resistance of the steel pipe prebored and precast piles based on field load-transfer curves and finite element method. *Soils Found*., 60, 478–495. doi:10.1016/j.sandf.2020.03.011.

[12] Krasiński, A.; Sieńko, R. (2010). Pomiar pionowego rozkładu siły w palu podczas testów statycznych. In Proceedings of the 56 Konferencja Naukowa Komitetu Inżynierii Lądowej i Wodnej PAN oraz Komitetu Nauki PZiTB, 161–168.

[13] Gwizdala, K.; Krasinski, A. (2013). Bearing capacity of displacement piles in layered soils with highly diverse strength parameters. Proc. 18th Int. Conf. Soil Mech. Geotech. Eng, 2739–2742.

[14] Sienko, R.; Bednarski, L.; Kanty, P.; Howiacki, T. (2019). Application of Distributed Optical Fibre Sensor for Strain and Temperature Monitoring within Continuous Flight Auger Columns. IOP Conf. Ser. *Earth Environ. Sci.*, 221. doi:10.1088/1755-1315/221/1/012006.

[15] Buda-Ożóg, L.; Zięba, J.; Sieńkowska, K.; Nykiel, D.; Zuziak, K.; Sieńko, R.; Bednarski, Ł. (2022). Distributed fibre optic sensing: Reinforcement yielding strains and crack detection in concrete slab during column failure simulation. *Meas. J. Int. Meas. Confed*., 195, doi:10.1016/j.measurement.2022.111192.

[16] Baca, M.; Rybak, J. (2021). Pile base and shaft capac-

ity under various types of loading. *Appl. Sci*., 11, doi:10.3390/app11083396.

[17] Zarkiewicz, K. (2019). Laboratory Experiment of Soil Vertical Displacement Measurement Near an Axially Loaded Pile. *IOP Conf. Ser. Mater. Sci. Eng*., 603, 032012, doi:10.1088/1757-899X/603/3/032012.

[18] Wang, Y.; Liu, X.; Sang, S.; Zhang, M.; Wang, P. (2020). A model test for the influence of lateral pressure on vertical bearing characteristics in pile jacking process based on optical sensors. *Sensors* (Switzerland), 20, doi:10.3390/s20061733.

[19] Lehane, B.M.; White, D.J. (2005). Lateral stress changes and shaft friction for model displacement piles in sand. *Can. Geotech. J*., 42, 1039–1052, doi:10.1139/t05-023.

[20] Żarkiewicz, K. (2019). Lateral stress changes along the pile skin during axial loading in laboratory test. In Proceedings of the Geotechnical Engineering foundation of the future; Reykjavik, 1–8.

[21] Konkol, J.; Bałachowski, L. (2017). Influence of Installation Effects on Pile Bearing Capacity in Cohesive Soils – Large Deformation Analysis Via Finite Element Method. *Stud. Geotech. Mech*., 39, doi:10.1515/sgem-2017-0003.

[22] Tovar-Valencia, R.D.; Galvis-Castro, A.; Salgado, R.; Prezzi, M.; Fridman, D. (2022). Experimental measurement of particle crushing around model piles jacked in a calibration chamber. *Acta Geotech*., 8, doi:10.1007/s11440-022-01681-8.

[23] Henke, S.; Grabe, J. (2006). Simulation of pile driving by 3-dimensional Finite-Element analysis. Proc. 17th Eur. Young Geotech. Eng. Conf.

[24] Haque, M.N.; Abu-Farsakh, M.Y.; Zhang, Z. (2020). Evaluation of pile capacity from CPT and pile setup phenomenon. *Int. J. Geotech. Eng*., 14, 196–205, doi:10.1080/19386362.2017.1413035.

[25] Eslami, A.; Valikhah, F.; Veiskarami, M.; Salehi, M. (2017). CPT-Based Investigation for Pile Toe and Shaft Resistances Distribution. *Geotech. Geol. Eng*., 35, 2891–2905, doi:10.1007/s10706-017-0287-8.

[26] Żarkiewicz, K. (2018). Laboratory research of toe resistance based on static pile load tests in different schemes. *Civ. Envionmental Eng. Reports*, 28, 80–81, doi:10.2478/ceer-2018-0014.

[27] Meyer, Z.; Żarkiewicz, K. (2017). Mechanizm formowania się oporu pobocznicy przy podstawie pala określony na podstawie badań laboratoryjnych. *Inżynieria i Bud.*, R. 73, nr 5.

[28] Żarkiewicz, K.; Meyer, Z. (2016). Nowe spojrzenie na współpracę pala z gruntem w świetle badań laboratoryjnych. Wiadomości Proj. Budownictwa, maj.

[29] Żarkiewicz, K.; Qatrameez, W. (2021). Assessment of Stress in the Soil Surrounding the Axially Loaded Model Pile by Thin, Flexible Sensors. *Sensors*, 21, doi:10.3390/s21217214.

[30] PN-EN ISO 14688-1:2018-05. Geotechnical investigation and testing – Identification and classification of soil – Part 1: Identification and description (ISO 14688-1:2017).

[31] Kamal, Z.A.; Arab, M.G.; Dif, A. (2016). Analysis of The arching phenomenon of bored piles in sand. *Alexandria Eng. J.*, 55, 2639–2645. doi:10.1016/j.aej.2016.06.035.